Energy Dissipation within the Wave Run-Up at Stepped Revetments

Nils B. Kerpen
Franzius-Institute, Leibniz Universität Hannover
kerpen@fi.uni-hannover.de

Daniel B. Bung
Hydraulic Engineering Section, Fachhochschule Aachen
bung@fh-aachen.de

Daniel Valero
Hydraulic Engineering Section, Fachhochschule Aachen
valero@fh-aachen.de

Torsten Schlurmann
Franzius-Institute, Leibniz Universität Hannover
schlurmann@fi.uni-hannover.de

Abstract

To understand the processes and performance of energy dissipation caused by turbulence during the wave run-up over a stepped revetment hydraulic model tests with steady flow conditions are conducted and correlated with unsteady flow conditions of the wave run-up within a short time frame. An analogy to the energy dissipation at stepped spillways is presumed. Under irregular waves the run-up reduction over a stepped revetment is dependent on the Iribarren number and decreases for decreasing Iribarren numbers. Velocity gradients are similar in a steady and unsteady flow regime near the pseudo-bottom.

Keywords: run-up, stepped revetment, roughness, energy dissipation

1. Introduction

Besides an ever increasing demand to optimize a robust protection level against storm surges, coastal protection structures in urbanized coastal areas need to allow unobstructed access to coastal waterfronts and meet architectural landscape aspects. Both issues can be granted by a stepped revetment. Former studies and resulting design guidelines merely analyzed the reduction of wave run-up and wave overtopping volumes over stepped revetments in physical model tests – most of them in regular waves and with a very limited variation of hydraulic and geometrical boundary conditions. [1] Hence, these investigations led to design criteria with a limited range of application.

In comparison to a smooth slope the turbulence over a stepped revetment is enlarged and the energy dissipation increased. Therefore, the run-up and overtopping values decrease. To understand and describe the process of energy dissipation during the wave run-up over a stepped revetment a new set of physical model tests is conducted. Selected flow conditions (varying flow velocities and layer thickness over each step) from the unsteady wave run-up tested in the wave flume 'Schneiderberg' at Franzius-Institute in Hannover are translated to a steady flow regime implemented in a current flume at the Hydraulic Engineering Section of University of Applied Sciences in Aachen. This methodology allows for a better understanding of underlying hydraulic processes. It is hypothesized that underlying processes from the steady-state tests mimic the unsteady wave run-up and help improving knowledge of wave run-up dissipation on stepped revetments. Therefore, velocity profiles along the water body and velocity gradients near the pseudo-bottom (formed by the outer edges of the steps) need to be comparable in order to assume similar flow resistances and energy dissipation rates, both being linked to the full wave run-up process. This paper aims to present first results from preliminary tests.

A notation overview is given in Figure 1. Next to commonly used hydraulic and geometry related parameters (water depth h_s, significant wave height H_{m0}, peak wave period T_p, wave run-up height R_u, foreshore slope i, structure slope n) two new parameters describing the step geometry are included with S_h representing the step height and S_w representing the step width.

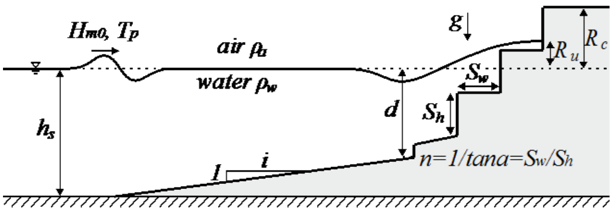

Figure 1. Notation overview of hydraulic and geometry related parameters of a stepped revetment.

2. State of the Art

Recent literature and guidelines ([2], [3]) give dimensionless design formulae (e.g. for run-up prediction on rough slopes) by

$$R_{u,2\%} / H_{m0} = A\gamma_f \xi_{m-1,0} \quad (1)$$

with $R_{u,2\%}$ depicting the run-up height exceeded by 2% of the incoming waves, H_{m0} the significant wave height, A as empirical contingent coefficient, γ_f as influence factor for roughness elements with

$$\gamma_f = R_{u,2\%,rough} / R_{u,2\%smooth} \quad (2)$$

and $\xi_{m-1,0}$ as breaker parameter. The parameter γ_f takes values in the magnitude of 1.0 for grass, 0.95 for basalt or 0.6 for single layer rocks over an impermeable core ([2]) while it underlies a wide spreading of $0.56 < \gamma_f < 0.9$ for stepped revetments ([4], [5], [6], [7], [8]). [4] started initially with run-up tests on composite slopes (smooth, rip-rap, vertical wall, stepped revetment). [5] summarized run-up tests conducted in the Netherlands for more than 20 years including two stepped geometries. [6] and [7] focused on the step geometry and its effect on the wave run-up. [8] listed reduction coefficients in comparison to alternative revetments. A comprehensive review of recent literature with respect to wave interaction with stepped revetments is given in [1]. It is known that for stepped revetments, γ_f decreases for milder slopes. A clear trend regarding the dependence of the wave height H_{m0} in relation to the step height S_h cannot be drawn on the basis of the present available data sets since underlying processes during wave run-up and run-down have never been thoroughly addressed in any study.

3. Methodology and experimental set-ups

To better understand the flow resistance generating processes during the wave run-up over a stepped revetment hydraulic model tests with steady flow conditions are conducted in a current flume at the Hydraulic Research Section at University of Applied Sciences in Aachen and correlated with unsteady flow conditions of the wave run-up in a wave flume at Franzius-Institute at Leibniz Universität Hannover.

In both setups, the flow is observed by a high speed camera (Phantom Miro M120 by *LaVision*) with a resolution of 1920 x 1200 px. The settings are summarized in Table 1. It must be noted that sample rate is limited for a given sample time due to internal storage capacity.

Table 1. High speed camera settings in both setups.

	Current flume	Wave flume
Sample rate [Hz]	732 Hz	200
Pixel density [px/cm]	30	33
Sample time [s]	5.00	1.37

Beside the qualitative analysis of the flow, the images are used to estimate velocity fields by application of the bubble image velocimetry (BIV) method introduced by [9]. Different from Particle Image Velocimetry (PIV), bubbles are considered as tracer particles assuming a slip-free air bubble transport. Applicability of this method to highly aerated stepped spillway flow has been demonstrated in several studies before (e.g. [10], [11], [12], [13]).

The images are evaluated in the MATLAB® toolbox PIVlab (1.41) developed by [14]. For cross-correlation, two passes are performed starting with interrogation window sizes of 64 x 64 px and 32 x 32 px, respectively. It must be noted that with a maximum velocity of about 1.5 m/s and the settings given in Table 1, the maximum particle displacement between two subsequent images is about 22 px in the wave flume and 6 px in the current flume, respectively. Overlap is set to 50 %. The structure is masked out to enhance calculation speed. In order to overcome the problem of possible incomplete velocity fields due to strong noise and resulting poor correlations, averaged velocity fields from multiple calculations will be presented below. In unsteady condition (i.e. in the wave flume), only 5 frame pairs are taken into account while in steady condition (i.e. in the current flume), 999 image pairs are considered.

3.1. Unsteady flow conditions

The wave flume has a width of 2.2 m, a length of 110 m and a maximum water depth of 1.0 m. The model was placed over horizontal ground in a distance of about 24.1 m to the piston wave maker operating with 2nd order wave generation routines. At this position in the flume an observation window in the side flume wall allows studying processes beneath the water surface and permitting the thorough analysis of wave run-up and overtopping processes. Details of the experimental set-up and test conditions are given in [15]. An impression of the set-up is given in Figure 2.

Tests for regular waves for five different wave heights $0.11 \text{ m} \leq H \leq 0.16 \text{ m}$, constant wave period $T = 2.0$s and constant water level $h_s = 0.995$ m in front of a foreshore berm have been conducted for two specific, but standard slope angles, i.e. 1:2 (30.0°) and 1:3 (19.7°). The water depth over the submerged foreshore berm at the toe of the stepped revetment $d = 0.5$ m is constant.

Figure 3 shows a single frame of an exemplary recording of the high turbulent and fully aerated flow regime over the stepped revetment within the wave run-up process.

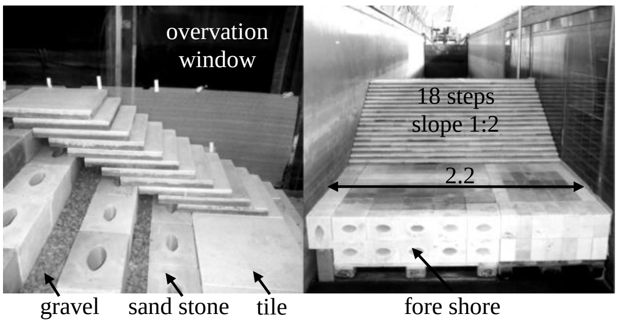

Figure 2. Set-up in the wave flume, measures in [m].

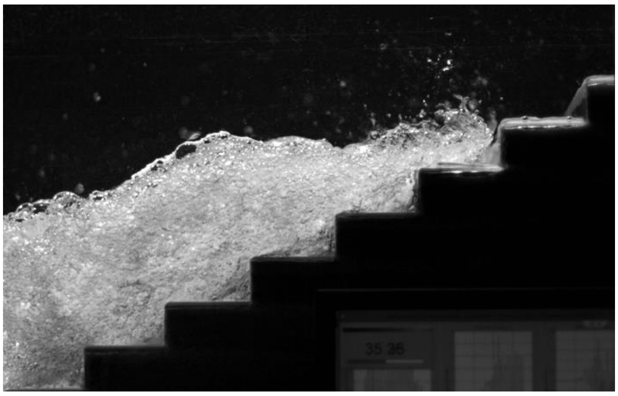

Figure 3. High speed frame taken in wave flume for T = 2.3 s and H = 0.15 m, wave propagation from left to right (note the strong aeration of the flow).

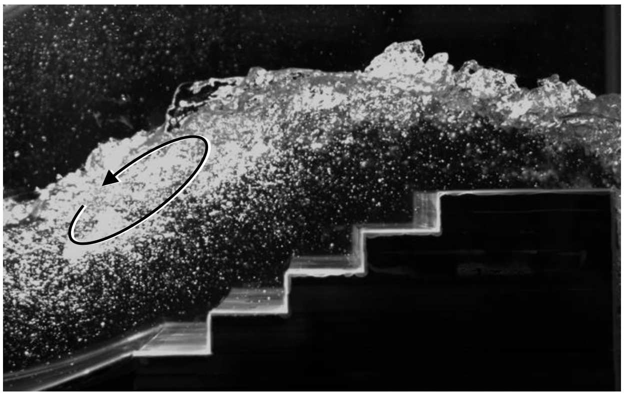

Figure 5. Exemplary frame of a high speed recording in the current flume for Q = 65 l/s, flow from left to right (note the strong aeration of the flow).

In a second configuration build by composite lumber sheets over horizontal floor a stepped revetment without foreshore and a homogeneous slope of 1:2 with 0.05 m step height was placed at a distance of 86 m from the wave board. At this set-up the wave reflection coefficient was determined for irregular waves (14 tests, each >1,000 waves) with $0.01 \leq H_{m0}/L_{m-1,0} \leq 0.067$.

3.2. Steady flow conditions

The current flume is 12.0 m long, 0.585 m wide and 0.8 m deep. The discharge can be progressively adapted by means a frequency-regulated pump to a maximum of 90 l/s. The model (Figure 4) is set-up by hard foam sheets bent to a ramp with a radius of 0.7 m over a length of 1.25 m followed by four steps with a height of 0.04 m and a slope of 1:2 made of PVC plates. The flow is formed by a sluice gate generating a water level giving sufficient energy head to overcome the stepped structure. The discharge has been varied stepwise (5 l/s) from 25 l/s ≤ Q ≤ 65 l/s. However, in this paper a single discharge condition with 65 l/s, a gate opening of 0.06 m and an upstream head of about 0.75 m is presented.

The flow depth perpendicular to the pseudo-bottom is measured over each step and upstream of the sluice gate is measured by ultrasonic sensors (mic+130/UI/TC by *microsonic*) for 30 s with a sampling rate of 50 Hz. Point measurements of flow velocities are conducted with a propeller (MiniWater6 Micro by *Schiltknecht*) and an ADV-probe (Vectrino Profiler by *Nortek*). Figure 5 shows a single frame of an exemplary recording. The reader may note the strong aeration of the flow. In the present study, sufficient aeration was found for discharges $Q \geq 50$ l/s.

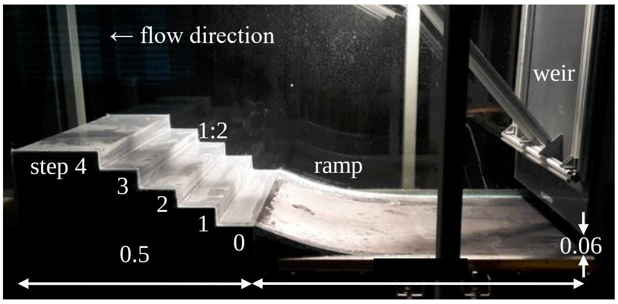

Figure 4. Set-up in the current flume, flow direction from right to left, measures in [m].

4. Results

The energy dissipation at a coastal protection structure such as a stepped revetment is influenced by many hydraulic and geometry related boundary conditions. For that reason a separation of global and local view on the energy dissipation is given subsequent in order to enable a deeper understanding of the driving parameter.

4.1. Global energy dissipation

To get an impression of the energy dissipation over a stepped revetment the wave run-up is closer analyzed. Figure 6 discusses the influence of the type of slope and wave breaking on the wave run-up. Therefore, the relative wave run-up height $R_{u2\%}/H_{m0}$ is given over the Iribarren number $\xi_{m-1,0}$. Three empirical approaches for plain slopes by [2], [3], and [15] are compared with the measured relative wave run-up of a stepped revetment

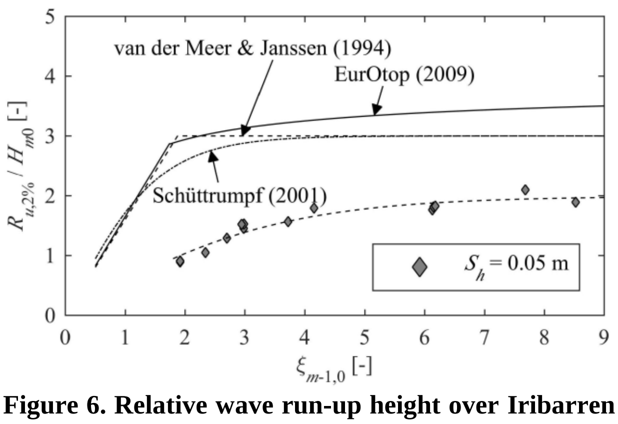

Figure 6. Relative wave run-up height over Iribarren number (plain slopes from literature and tested stepped slope).

with a relative step height of $0.56 < S_h/H_{m0} < 0.91$.

For all slopes the relative wave run-up increases with an increasing Iribarren number or correspondingly a decreasing wave steepness or increasing slope angle. Due to the higher turbulence within the run-up process over a stepped revetment in comparison to plain slopes more energy is dissipated. Thus, the run-up is reduced significantly for a wide range of Iribarren numbers ($1.8 < \xi_{m-1,0} < 9$).

The measured relative wave run-up heights given in Figure 6 can be represented by a hyperbolic tangent best fit regression following the relation

$$R_{u,2\%} / H_{m0} = 2.0 \tanh\left(0.29\xi_{m-1,0}\right). \qquad (3)$$

The quality of this regression is discussed in Figure 7. Values calculated by (3) are given over the measured values. With a coefficient of determination of $R^2 = 0.93$ and a standard deviation of $STD = 0.102$ a strong correlation is approved.

To determine the reduction coefficient γ_f for this stepped revetment corresponding run-up values will be normalized with the run-up over a smooth revetment by following (2). Due to the validity of [1] for wave run-up in a wide range of Iribarren numbers ($0.5 < \xi_{m-1,0} < 8$) this empirical derived approach is chosen as reference for irregular wave run-up over plain slopes leading to

$$\gamma_f = 2.0 \tanh\left(0.29\xi_{m-1,0}\right) / \left(4 - 1.5\xi_{m-1,0}^{-0.5}\right). \qquad (4)$$

In Figure 8 the reduction coefficient γ_f depicting the wave run-up reduction of irregular waves over a stepped revetments is given with respect to the Iribarren number. The coefficient increases with an increasing Iribarren number. Hence, the energy dissipation decreases for more gentle wave steepness or steeper slopes.

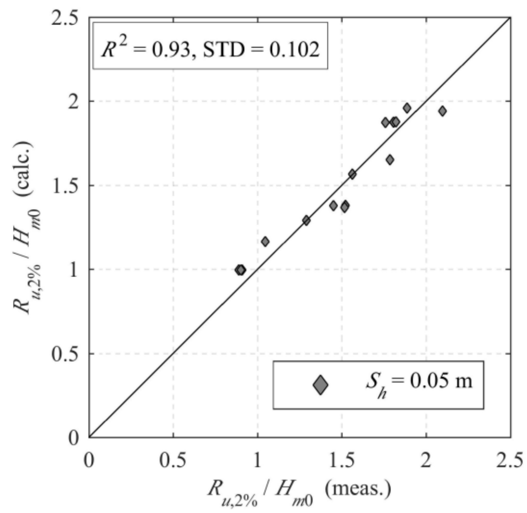

Figure 7. Regression quality.

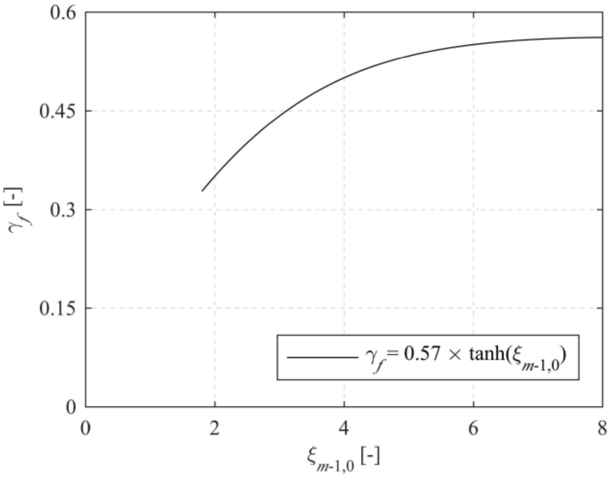

Figure 8. Reduction coefficient γ_f over Iribarren number.

4.2. Local effects on the energy dissipation

To draw a deeper understanding of the driving mechanism of energy dissipation over stepped revetments hydraulic flow pattern will be analyzed for various conditions.

4.2.1. Qualitative comparison. It may be observed that the wave run-up is much more aerated than the steady flow in the current flume when comparing the high speed frames in Figure 3 and 5. The high aeration in the wave flume is caused by the strong impact of the wave on the steps while aeration in the current flume is due to a surface roller close to the gate. This roller releases air bubbles occasionally to the flow. However, these air bubbles rarely reach lower flow regions close to the pseudo-bottom. Nevertheless, the flow is sufficiently aerated for application of BIV.

In terms of comparability, it may be concluded that friction near the pseudo-bottom is reduced in case of the wave due to this high air content in this shear region. The roller in the current flume, i.e. a hydraulic jump transferring the supercritical to subcritical flow does not allow interpretation for the first steps while the flow is redirected to the horizontal on the fourth flow. For this preliminary study, data taken on the second step only are taken into account. Here, the flow is almost unaffected by the roller and aligned with the pseudo-bottom.

4.2.2. Flow velocities. Full velocity fields from BIV are shown in Figure 9. Detailed plots of the velocity fields on step 8 for the wave flume and step 2 for the current flume are shown in Figure 10. Figure 9a emphasizes that 6 frame pairs are not sufficient to obtain smooth velocity fields and thus, reliable results, and supports the need of additional steady-state experiments to investigate energy dissipating processes.

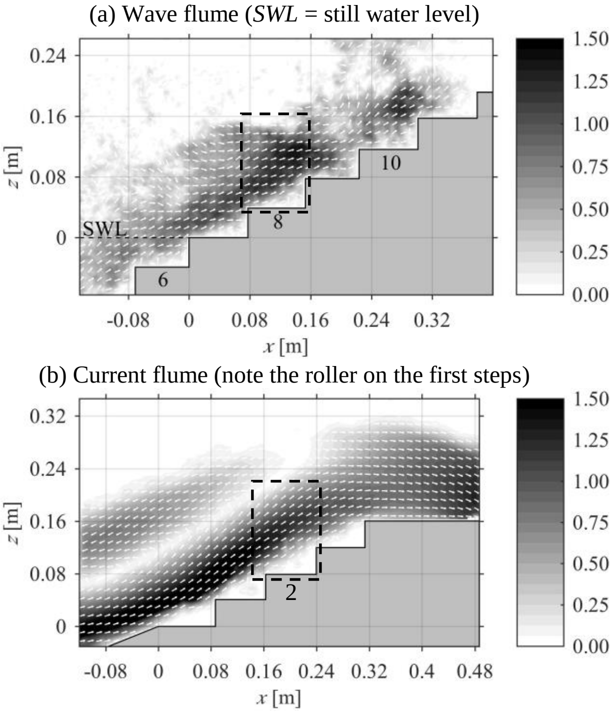

Figure 9. Velocity fields in [m/s] for the full fields of view and both setups (only every 5*th* vector is displayed; vector lengths are normalized for better legibility).

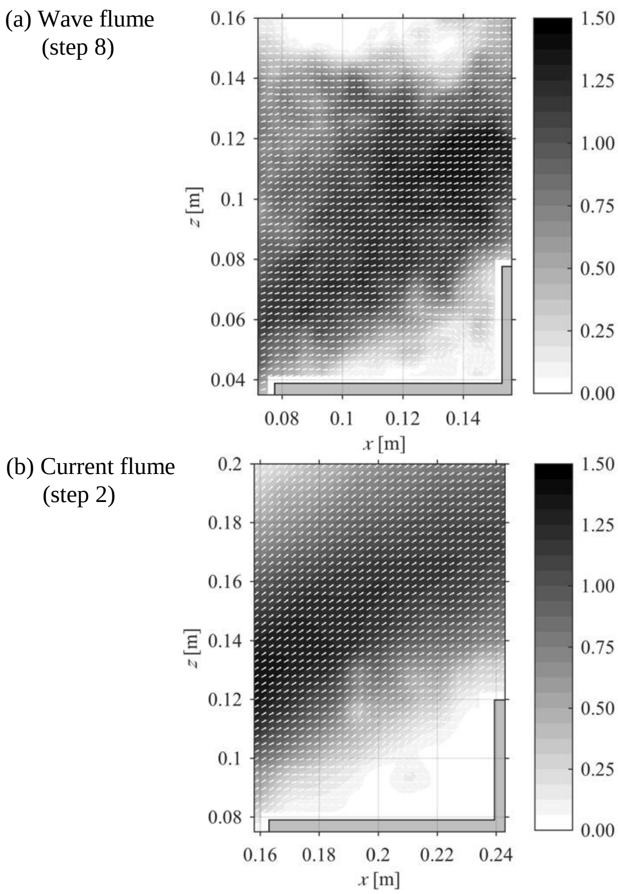

Figure 10. Velocity fields in [m/s] for selected steps and both setups (only every 5th vector is displayed; vector lengths are normalized for better legibility).

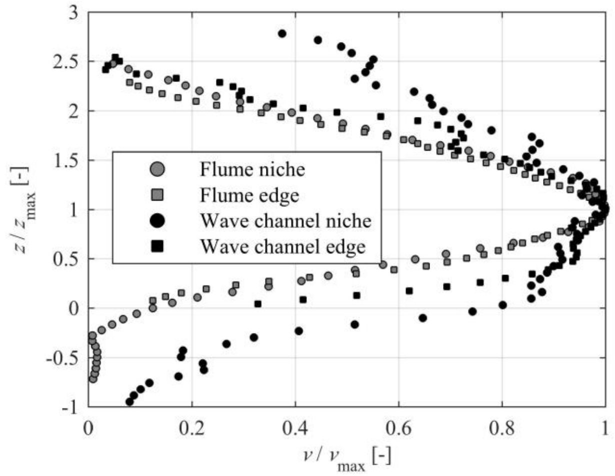

Figure 11. Normalized velocity distributions at upstream step edges and over the step niche (z = 0 at the pseudo-bottom), step 8 for the wave channel and step 2 for the current flume (see Figure 9).

Yet, detailed plots in Figure 10 demonstrate that velocity fields are similar in terms of qualitative distribution, direction as well as magnitudes close to the pseudo-bottom. Within the step cavity, velocity distributions differ slightly. It is assumed that the more chaotic distribution in the wave flume are due to the strong and complex wave impact during the run-up.

Normalized velocity distribution at the upstream step edges as well as over the step niche are shown in Figure 11. As it was pointed out before, the velocity profiles compare fairly well, except for the step niche in the wave flume where velocities are higher within the cavity. Anyway, it is observed that velocity gradients are similar near the pseudo-bottom. It may thus be assumed that the flow resistance generated within the shear region is similar for both setups.

5. Conclusion

The energy dissipation over a stepped revetment has been analyzed for irregular waves (unsteady flow conditions) in a wave flume and under idealized steady flow conditions in a current flume. Result of the analysis of the unsteady flow conditions under waves was a decreasing energy dissipation for gentler wave steepness or steeper slopes. A formula calculating the reduction coefficient of a stepped revetment dependent on the Iribarren number was empirically derived.

Acknowledgements

The present work is part of the joint research project 'waveSTEPS' funded by the German Federal Ministry of Education and Research (BMBF) through the German Coastal Engineering Research council (KFKI, 03KIS108 and 03KIS119). The authors gratefully acknowledge the support of the experimental work by Kornelius Müller within the wave flume experiments and Jochen Vogel within the current flume experiments.

6. References

[1] N.B. Kerpen und T. Schlurmann, „Stepped revetments - revisited," in *Proceedings of the 6th international conference on application of physical modelling in coastal and port engineering and science*, Ottawa, Canada, 2016.

[2] KFKI, European Overtopping Manual, vol. 73, Heide i. Holstein: Boyens Mediean GmbH & Co. KG, 2007.

[3] J. van der Meer and J. Janssen, "Wave run-up and wave overtopping at dikes," in *Wave Forces on Inclined and Vertical Structures*, ASCE, 1995, pp. 1-27.

[4] T. Saville, "Wave run-up on composite slopes," *Proceedings of the 6th conference on coastal engineering,* pp. 691-699, 1957.

[5] F. Wassing, „Model investigations on wave run-up carried out in the Netherlands during the past twenty years," *Proceedings of the 6th international conference on coastal engineering,* pp. 700-714, 1957.

[6] R. Jachowski, „Interlocking precast concrete block sea wall," *Proceedings of the 9th conference on coastal engineering,* pp. 504-517, 1964.

[7] P. Nussbaum und B. Colley, „Dam construction and facing with soil cement," *Bulletin RD 010.01W, Portland cement assosiation,* p. 111, 1971.

[8] B. McCartney, „Survey of coastal revetment types," *Coastal engineering research center,* Bde. 1 von 276-7, 1976.

[9] Y. Ryu, K.-A. Chang & H.-J. Lim. Use of bubble image velocimetry for measurement of plunging wave impinging on structure and associated greenwater, *Meas. Sci. Technol.*, 16 (10), 2005, pp. 1945-1953.

[10] D.B. Bung. Non-intrusive measuring of air-water flow properties in self-aerated stepped spillway flow. *34th IAHR World Congress*, Brisbane, 2011, pp. 2380-2387.

[11] J. Leandro, D.B. Bung, & R. Carvalho. Measuring void fraction and velocity fields of a stepped spillway for
ming flow using non-intrusive methods. *Experiments in Fluids*, 55(5), 2014.

[12] D.B. Bung & D. Valero. Image processing for Bubble Image Velocimetry in self-aerated flows, *36th IAHR World Congress*, Den Haag, 2015.

[13] D.B. Bung & D. Valero. Image processing techniques for velocity estimation in highly aerated flows: Bubble Image Velocimetry vs. Optical Flow, *4th IAHR Europe Congress*, Liege, 2016.

[14] W. Thielicke & E.J. Stamhuis. PIVlab – Towards user-friendly, affordable and accurate digital Particle Image Velocimetry in MATLAB. *Journal of Open Research Software* 2(1): e30, 2014.

[15] H.F. Schüttrumpf. Wellenüberlaufströmung bei Seedeichen: Experimentelle und theoretische Untersuchungen, *volume 149 of Mitteilungen aus dem Leichtweiß Institut für Wasserbau. Braunschweig, 2001*.

[16] N.B. Kerpen and T. Schlurmann, "Experimental inestigation on wave overtopping on stepped embankments," *Proceedings of the 5th international conference on application of physical modelling to port and coastal protection,* vol. 1, pp. 262-269, 2014.